ELSEVIER

Journal of Organometallic Chemistry 549 (1997) 203–212

Journal of Organometallic Chemistry

Crystal structure, conformational diversity and solution NMR spectroscopy of four tris(indenyl) lanthanoid(III) tetrahydrofuran adducts: $[Ln(C_9H_7)_3 \cdot THF]$ (Ln = La, Pr, Nd, Sm)

Jingwen Guan [a], Qi Shen [b], R. Dieter Fischer [a,*]

[a] *Institut für Anorganische und Angewandte Chemie, Universität Hamburg, Martin-Luther-King-Platz 6, Hamburg D-20146, Germany*
[b] *Faculty of Chemistry and Chemical Engineering, Suzhou University, Suzhou 215006, P.R. China*

Received 10 June 1997; received in revised form 30 July 1997

Abstract

Four homologous tris(indenyl)lanthanoid(III) adducts, $[Ln(C_9H_7)_3THF]$ (THF = tetrahydrofuran), with Ln = La (**1**), Pr (**2**), Nd (**3**) and Sm (**4**) were prepared in excellent yields, and six single crystals, **1a**, **1b**, **2**, **3a**, **3b** and **4** (**1** and **3** being at least dimorphic) have been subjected to detailed X-ray studies. The C_5-fragments of the C_9H_7 ligands are almost pentahapto-bonded, and either two or three C_9H_7 units adopt paddle-wheel-like orientations. The crystals **1a**, **2** and **3a** contain *two* molecules of different conformation, one molecule displaying one C_9H_7 benzo group in a transoid orientation relative to the THF ligand. A similar conformation, albeit with one cisoid benzo group, is realized in **1b**. Three characteristic structural motifs, I (**1a**, **2**, **3a**), II (**1b**) and III (**3b**, **4**), emerge from the present results, and appear to be consistent with earlier findings. Motif III is most remarkable in view of its hexagonal, chiral space group $P6_3$, owing to 'trigonally disordered' THF units. Solution ^1H NMR spectroscopy indicates three rapidly equilibrating virtually equivalent C_9H_7 ligands, the ^{139}La NMR spectrum of **1** and the MCD spectrum of **2** admitting again η^5-coordination. The long-pending suggestion of predominantly η^1-coordinated C_9H_7 ligands in dissolved molecules of **4** seems to be no longer justified. © 1997 Elsevier Science S.A.

Keywords: Indenyl ligand; Lanthanoid complexes; THF adducts; Crystal structure; Solution NMR (^1H, ^{139}La)

1. Introduction

While the structural chemistry of the mainly polymeric, base-free tris(cyclopentadienyl) complexes of the rare earth elements, $[Ln(C_5H_5)_3]$, has turned out to be surprisingly diverse [1–4], the corresponding tetrahydrofuran adducts, $[Ln(C_5H_5)_3 \cdot (THF)]$, are structurally quite uniform [5–8]. [1] A somewhat reverse situation might, on the other hand, hold for the base-free tris(indenyl) complexes, $[Ln(C_9H_7)_3]$, and their THF adducts $[Ln(C_9H_7)_3 \cdot (THF)]$, respectively. While the space-demanding benzo groups of the three indenyl ligands efficiently prevent poly- or oligomerization of the THF-free molecules [9], [2] various conformers are, in principle, possible both for molecules of the base-free complexes ([2]) and for their adducts $[Ln(C_9H_7)_3L]$ (L = Lewis base). The different conformers of the latter may best be distinguished by the actual orientations of the vectors connecting the centres of the five- and six-membered ring of each C_9H_7 unit relative to the direction of the Ln–L bond [10]. Interestingly, some of these conformers should even be chiral, and crystals containing just one enantiomorphic $[Ln(C_9H_7)_3 \cdot (THF)]$ molecule have recently been described [11]. Although two contributions considering the attractive structural chemistry of $[Ln(C_9H_7)_3 \cdot (THF)]$ systems with Ln = Pr (**2a** [12]), Nd (**3c** [11]) and Gd (**5** [11]) have appeared, it should be recalled that all single crystals studied so far were obtained as *by-products* of reactions initially designed for different goals. There is, moreover, some dearth of information on characteristic spectroscopic (e.g., NMR-, NIR/VIS- and MCD) properties of well-defined $[Ln(C_9H_7)_3 \cdot (THF)]$ systems in solution. So far, mainly a few interesting results reported in a PhD Thesis [13] may be considered in addition to earlier, at least partially erroneous (vide infra) NMR-studies

* Corresponding author.

[1] Comprehensive review: Ref. [4].

[2] According to recent unpublished work (J. Guan, R.D. Fischer), the deep red, base-free Pr-complex is not isostructural with its earlier-studied Sm-homologue (Ref. [9]).

PII S0022-328X(97)00565-2

[14,15]. One combined NIR/VIS-MCD study of **2** in 2-methyltetrahydrofuran was, moreover, published in 1986 [16]. Another essential objective of the present work has, therefore, been to establish satisfactory, straightforward syntheses of the generally quite labile tris(indenyl)metal complexes.

2. Synthesis and general properties of 1–4

In principle, the preparation of the title complexes $[Ln(C_9H_7)_3 \cdot (THF)]$ corresponds to procedures already described in the literature [13–17]:

$$LnCl_3 + 3NaC_9H_7 \xrightarrow{THF} [Ln(C_9H_7)_3 \cdot THF] + 3NaCl$$

However, one apparently crucial improvement has been that the reaction mixture was kept refluxing in THF for at least three days. When, after NaCl-removal and drying, the crude residue was extracted with a large amount of hot toluene, very pure $[Ln(C_9H_7)_3 \cdot (THF)]$ could be isolated in excellent yields (Table 1) from the concentrated, and subsequently cooled, mother liquor. In this way, the formation of otherwise substantial *by-products* could be strictly avoided. According to earlier reports [18–20], binuclear systems of the type: $[M(THF)_6][Ln_2(C_9H_7)_6(\mu\text{-}Cl)]$ (Ln = Pr, Nd, Sm) have frequently accompanied the mononuclear THF adduct. Single crystals of the title complexes of excellent quality could be obtained by repeated recrystallization from toluene/THF mixtures.

All complexes are strongly air sensitive, their initial colours (see Table 1) turning instantaneously black when exposed to air. **1–4** are well-soluble in THF and CH_2Cl_2, reasonably well in C_6H_6, somewhat less satisfactorily in toluene, but insoluble in hexane. The most characteristic infrared (IR) bands of the C_9H_7 ligands occur at 3036, 1013, 864 and 765 cm^{-1}, and of the THF ligands at 1068 and 915 cm^{-1} [11,19,21]. In the mass spectra, pronounced metal-containing fragments of **1** with m/e = 371 and 372 correspond to $[La(C_9H_7)_2H_2]^+$; fragments of **2** with m/e = 486, 373 and 256 to $[Pr(C_9H_7)_n]^+$ (n = 3, 2, 1); fragments of **3** with m/e = 374, 375, 377 and 379 to $[Nd(C_9H_7)_2]^+$, and with m/e = 257, 259, 261 and 265 to $[Nd(C_9H_7)]^+$, respectively. Moreover, only a large number of peaks indicative of metal-free fragments was observed.

Removal of all THF from **2** requires higher temperatures than stated in [15]. Thus, from the red product obtained from **2** in vacuo at $< 1.0 \times 10^{-3}$ mbar and at ca. 90–100°C after 8 h, green crystals of **2** could be grown as the main product, as proved by elemental analysis, ^1H NMR and a single crystal X-ray study indicating a crystal isomorphous with crystal **2** (vide infra). All THF could actually be completely removed in vacuo ($< 1.0 \times 10^{-3}$ mbar) at temperatures slightly above 120°C after at least 5 h ([2]).

3. Crystal structures and molecular conformations of 1–4

Both **1** and **3** turned out to be at least dimorphic, since two different types of crystals (**1a/1b** and **3a/3b**, respectively) could be crystallographically distinguished. Consequently, six individual single crystals, corresponding to the samples **1a**, **1b**, **2**, **3a**, **3b** and **4**, were subjected to detailed X-ray studies. A third crystal of compound **1** (**1c**) [Shen et al., unpublished] with structural data very similar to those of **1a** was investigated, too, but will not be considered in more detail in this paper. Each crystal involves individual $[Ln(C_9H_7)_3 \cdot (THF)]$ molecules with three approximately η^5-bonded C_5-units of the C_9H_7 ligands, in accordance with quasi-tetrahedral coordination. Selected bond lengths and angles listed in Table 3 compare well with earlier reported data [10–12]. Moreover, the usual consequences of the decrease of the ionic radius of the Ln^{3+} ion when moving from La^{3+} to Sm^{3+} are clearly reflected (e.g., by a concomitant shortening of the average Ln–C and Ln–O distances). In accordance with earlier observations [10–12,18–20], the two carbon atoms shared by both the C_5 and C_6 fragments of a

Table 1
Yields, elemental analyses, colours and melting points of **1–4**

Complex (Ln)	Yield (%)	Elemental analysis (calculated values)			Physical properties	
		C	H	Ln	Colour	m.p. (°C)[a]
1 (La)	89	66.42 (66.93)	5.26 (5.21)	25.07 (24.97)	colourless	168–172
2 (Pr)	78	65.48 (66.69)	5.27 (5.19)	24.37 (25.24)	yellowish green	173–178
3 (Nd)	80	65.41 (66.30)	5.22 (5.16)	25.38 (25.68)	green	179–185
4 (Sm)	75	65.35 (65.58)	5.21 (5.10)	25.64 (26.48)	deep red	204–208

[a] Partial decomposition.

C_9H_7 ligand lie significantly more remote from the metal ion than the three carbon atoms belonging exclusively to the C_5 fragment which are likely to approach a more allyl-like nature. However, since La–C distances as long as ca. 300 pm seem to contribute to metal-to-ligand bonding in $[La(C_5H_5)_3]_\infty$ [22], it maybe not straightforwardly be justified to consider the indenyl ligands of **1–4** as predominantly η^3-coordinated.

Table 2 presents the crystal data of all six samples and a survey of features on data collection and refinement. Focusing on the space groups, as well as on the values of *a*, *b*, *c* and *Z*, respectively, three different structural motifs may be distinguished. Motif I which is realized in the structures of **1a**, **2**, and **3a** is particularly complicated in that each crystal involves two non-equivalent molecular conformations as depicted in Fig. 2. Molecule (a) displays *three* paddle-wheel-like C_9H_7 ligands whose $C_5 \rightarrow C_6$ vectors (connecting the centre of the C_5 fragment with that of the adjacent C_6 fragment) lie approximately in one 'equatorial' plane of the complex (perpendicular to the Ln–O bond, see Fig. 1a and Table 4). In molecule (b), only two C_9H_7 ligands may be considered as paddle-wheel-like, while the $C_5 \rightarrow C_6$ vector of the third C_9H_7 ligand is oriented approximately parallel to the Ln–O bond, the benzo group being positioned transoid to the THF ligand (see Fig. 1b and Table 4). One precedent of conformation (a) is the adduct $[La(C_9H_7)_3TPPO]$ (TPPO = triphenylphosphinoxide [10]), while the corresponding methyl-tolyl-sulphoxide (MTSO) adduct [10] is configured similar to conformation (b). Motif I turns out to be realized also in **1c** and in a crystal of **2** examined recently by Ye et al. (i.e., sample **2a**, [12]). When the different designation of the crystallographic axes used by these authors is appropriately accounted for, the structural data of **2a** can be satisfactorily correlated with those of **2**.

Motif II involves only one type of molecule (Fig. 3), all three indenyl ligands of which adopt, however, different orientations. One of them lies almost equatorial (i.e., paddle-wheel-like), the second practically axial (i.e., parallel to the La–O bond) and the third one in an essentially intermediate position (see Fig. 1c). This situation may be quantified best by the set of individual distances of the three C_6-centres from the plane spanned by the three C_5-centres (see Table 4).

Interestingly, in motif II the benzo group of the quasi-axial C_9H_7 ligand lies cisoid with respect to the THF ligand. Precedents of this particular conformer which should suffer more strongly of steric congestion have, to the best of our knowledge, not been reported.

Motif III involves virtually one conformation (Fig. 4) whose three crystallographically equivalent C_9H_7 ligands generate $C_5 \rightarrow C_6$ vectors surround the Ln^{3+} ion clockwise in the 'equatorial plane' (spanned by the three C_5 centres, viewed from O to Ln; see Fig. 1d and Table 4). In motif III, each $\{(C_9H_7)_3LnO\}$ fragment adopts local C_{3v} symmetry, although the shape of the

Table 2
Survey of crystal data and details of data collection and refinement for the six samples of **1–4** investigated

	1a	**1b**	**2**	**3a**	**3b**	**4**
Formula weight	556.45	556.45	558.45	561.78	561.78	567.89
Temperature (K)	293(2)	293(2)	293(2)	293(2)	153(2)	293(2)
Diffractometer	Syntex $P2_1$	Syntex $P2_1$	Syntex $P2_1$	Syntex $P2_1$	Y290	Syntex $P2_1$
Wavelength (pm)	71.073	71.073	71.073	71.073	71.073	71.073
Crystal system	monoclinic	monoclinic	monoclinic	monoclinic	hexagonal	hexagonal
Space group	$P2_1/c$	$P2_1/c$	$P2_1/c$	$P2_1/c$	$P6_3$	$P6_3$
Unit cell dimensions (pm)	*a* 2370.7(7)	874.6(1)	2369.4(9)	2367.4(8)	1176.8(4)	1184.9(2)
	b 1060.9(1)	1986.8(8)	1053.2(1)	1053.6(3)	1176.8(4)	1184.9(2)
	c 2189.2(6)	1402.7(2)	2191.3(8)	2191.7(10)	1023.9(6)	1027.7(3)
	β 114.61(2)°	94.48(1)°	114.72(3)°	114.78(3)°		
Volume (nm^3)	5.006(2)	2.430(1)	4.965(3)	4.963(3)	1.2280(9)	1.2496(5)
Z	8	4	8	8	2	2
Density (calc., g cm^{-3})	1.477	1.521	1.494	1.504	1.519	1.509
Absorption coefficient (mm^{-1})	1.727	1.779	1.983	2.113	2.135	2.370
F(000)	2240	1120	2256	2264	566	570
θ Range for data collection (°)	2.54–27.56	2.34–27.57	2.55–27.57	2.55–22.55	2.82–30.08	2.81–27.52
Index ranges	*h* −29 to 28	−5 to 11	−29 to 28	−24 to 23	−2 to 15	−1 to 13
	k −13 to 1	−6 to 25	−13 to 1	−11 to 1	−2 to 15	−4 to 13
	l −1 to 26	−18 to 18	−12 to 26	−1 to 22	−14 to 14	−13 to 13
Reflections collected	13618	8514	13344	8261	3483	2734
Independent reflections (R_{int})	11330(0.0441)	5613(0.0351)	11321(0.0311)	6493(0.0465)	2417(0.0415)	1935(0.0473)
Data/restraints/parameters	11325/0/595	5612/0/298	11321/0/606	6471/9/596	2417/7/126	1935/2/114
Goodness of fit on F^2	1.056	1.128	1.105	1.147	1.063	1.065
Final *R* indices $[I > 2\sigma(I)]R_1/wR_2$	0.0812/0.2229	0.0347/0.0830	0.0712/0.1611	0.1103/0.2853	0.0343/0.0903	0.0436/0.1027
R indices (all data) R_1/wR_2	0.1214/0.2676	0.0431/0.0889	0.1130/0.1907	0.1194/0.3015	0.0354/0.0915	0.0568/0.1106
Largest diff. peak and hole (e nm^{-3})	3612 and −2137	1310 and −1071	2213 and −3278	2900 and −1897	1262 and −643	1484 and −883

axial THF ligand would not straightforwardly allow the Ln–O vector to function as a trigonal axis. Strict 'trigonal disorder' of the $\{C_4H_8\}$ fragments of all THF molecules in the crystal must, therefore, be accounted for. Xia et al. [11] have already described this remarkable crystallographic phenomenon.

Table 3
(a) Interatomic distances (in pm); and (b) significant bond angles (in deg.) of **1–4**

	1a	1b	2	3a	3b	4
Bond distance (pm)						
Ln–O	258.8(9)	257.5(2)	255.7(7)	258(2)	251.2(7)	249.4(11)
Ln–C(101)/(1)	281.2(11)	286.9(4)	274.5(9)	275(2)	276.2(4)	275.4(9)
Ln–C(102)/(2)	277.3(11)	280.9(3)	272.4(8)	271(2)	269.3(4)	266.7(8)
Ln–C(103)/(3)	284.6(11)	283.0(3)	280.2(8)	278(2)	273.6(5)	270.5(9)
Ln–C(108)/(8)[c]	*302.8(11)*	*298.8(3)*	*299.8(9)*	*300(2)*	*296.2(4)*	*296.3(8)*
Ln–C(109)/(9)	*303.7(10)*	*295.4(3)*	*300.1(8)*	*296(2)*	*296.5(4)*	*296.7(8)*
Ln–Ct(15)[a]	263.9	262.8	259.1	257	255.3	253.8
Ln–C(111)/(11)	281.2(14)	287.3(4)	278.8(10)	268(2)		
Ln–C(112)/(12)	276.7(13)	282.7(4)	271.6(9)	273(2)		
Ln–C(113)/(13)	284.7(13)	284.9(4)	277.4(10)	276(2)		
Ln–C(118)/(18)	*298.4(12)*	*302.7(3)*	*297.0(9)*	*293(2)*		
Ln–C(119)/(19)	*300.3(12)*	*298.8(3)*	*298.7(9)*	*294(2)*		
Ln–Ct(25)	261.8	265.1	257.9	256		
Ln–C(121)/(21)	285.2(12)	283.4(3)	282.1(10)	280(2)		
Ln–C(122)/(22)	280.0(13)	279.9(4)	275.7(9)	271(2)		
Ln–C(123)/(23)	279.5(12)	287.6(4)	277.8(10)	277(3)		
Ln–C(128)/(28)	*298.7(12)*	*298.3(3)*	*297.2(9)*	*297(3)*		
Ln–C(129)/(29)	*298.3(12)*	*301.3(3)*	*296.0(10)*	*296(3)*		
Ln–Ct(35)	262.0	264.1	259.7	257		
Ln*–O[b]	257.3(10)		254.3(7)	256(2)		
Ln*–C(201)	284.9(12)		282.0(10)	278(2)		
Ln*–C(202)	279.4(13)		274.5(9)	274(2)		
Ln*–C(203)	282.7(11)		277.3(9)	275(2)		
Ln–C(208)*	*299.8(11)*		*298.7(9)*	*308(2)*		
Ln–C(209)*	*298.2(13)*		*296.6(9)*	*299(3)*		
Ln*–Ct(15)	263.3		259.6	260		
Ln*–C(211)	289(2)		284.9(12)	285(3)		
Ln*–C(212)	282(2)		275.8(12)	272(4)		
Ln*–C(213)	277(2)		273.1(12)	271(4)		
Ln–C(218)*	*296.7(14)*		*292.7(12)*	*295(3)*		
Ln–C(219)*	*286.5(14)*		*284.0(11)*	*279(3)*		
Ln*–Ct(25)	260.1		256.2	254		
Ln*–C(221)	281.6(11)		276.4(11)	274(2)		
Ln*–C(222)	282(2)		275.1(11)	276(2)		
Ln*–C(223)	289(2)		284.5(10)	269(3)		
Ln–C(228)*	*299.4(13)*		*298.0(10)*	*293(3)*		
Ln–C(229)*	*304.4(12)*		*302.1(10)*	*300(3)*		
Ln*–Ct(35)	265.8		260.9	258		
Angles [°]						
O–Ln–Ct(15)	104.1	97.4	104.7	104.2	101.5	101.9
O–Ln–Ct(25)	99.1	103.0	98.6	99.7	101.5	101.9
O–Ln–Ct(35)	100.1	101.9	100.1	99.6	101.5	101.9
Ct(15)–Ln–Ct(25)	115.4	116.4	115.6	114.7	116.2	115.9
Ct(25)–Ln–Ct(35)	119.0	115.7	119.0	119.2	116.2	115.9
Ct(35)–Ln–Ct(15)	114.7	117.7	114.5	115.2	116.2	115.9
O–Ln*–Ct(15)	101.1		100.8	100.7		
O–Ln*–Ct(25)	98.3		98.6	99.1		
O–Ln*–Ct(35)	98.1		98.8	99.4		
Ct(15)–Ln*–Ct(25)	118.7		118.7	118.3		
Ct(25)–Ln*–Ct(35)	117.4		117.7	117.7		
Ct(35)–Ln*–Ct(15)	116.5		115.8	115.6		

[a] Ct means the centre of a five- or six-membered ring of the C_9H_7 ligand.
[b] Ln* designates molecules of type b of motif I (see the text).
[c] The bridged atoms which belong to the five- and six-membered rings and the distances of them to the Ln.

4. Discussion of the structural results

We have pointed out earlier [10] that most of the potential conformations of $[Ln(C_9H_7)_3L]$ adducts should be dissymmetric. Accordingly, the three different molecular conformations verified in the motifs I (two conformers) and II (one conformer) displaying either two or three paddle-wheel-like C_9H_7 ligands must occur as racemic mixtures, as the samples **1a**, **1b**, **1c**, **2** and **3a** crystallize all in the achiral space groups $P2_1/c$ or $P2_1/a$ (Table 6). Hence, in these samples, paddle-wheel-like structures of both clockwise and anti-clockwise arrangement are present in each individual crystal. On the other hand, *four* different samples (**3b**, **4**; **3c** [11] and **5** [11]) have by now independently been found to crystallize in the chiral space group $P6_3$. In these four representatives of motif III, each single crystal involves only one distinct enantiomeric molecule. Even more surprisingly, in all four crystals the paddle-like benzo groups of the three C_9H_7 ligands have been found to be oriented exclusively clockwise, when the molecule is viewed along its O–Ln axis from O to Ln.

A brief survey of all structural work carried out so far on $[Ln(C_9H_7)_3$ THF] systems is given in Table 6. Obviously, the two motifs I and III have been met most frequently. With some caution, one might deduce from these results that motif III is likely to become superior to motif I as the ionic radius of Ln(III) decreases. Interestingly, three samples of **2** (Ln = Pr) displaying exclusively motif I have been prepared and identified independently, whereas, on the other hand, two samples of complex **3** representing both motif III have been arrived at and investigated in two different laboratories. The convenient access of strictly enantiomorphic crystals at least of **3**, **4** and **5** provides an attractive chance to attempt more detailed chiroptic studies of novel solid chromophors involving 4f electrons. In particular, circularly polarized luminescence (CPL) spectroscopy of chiral Ln-complexes has become a promising research field with some interesting aspects of application [23].

5. Solution studies

5.1. ^{1}H- and ^{139}La-NMR spectroscopy

The 200 MHz ^{1}H-NMR spectra of **1–4** dissolved in C_6D_6 have in common that at room temperature

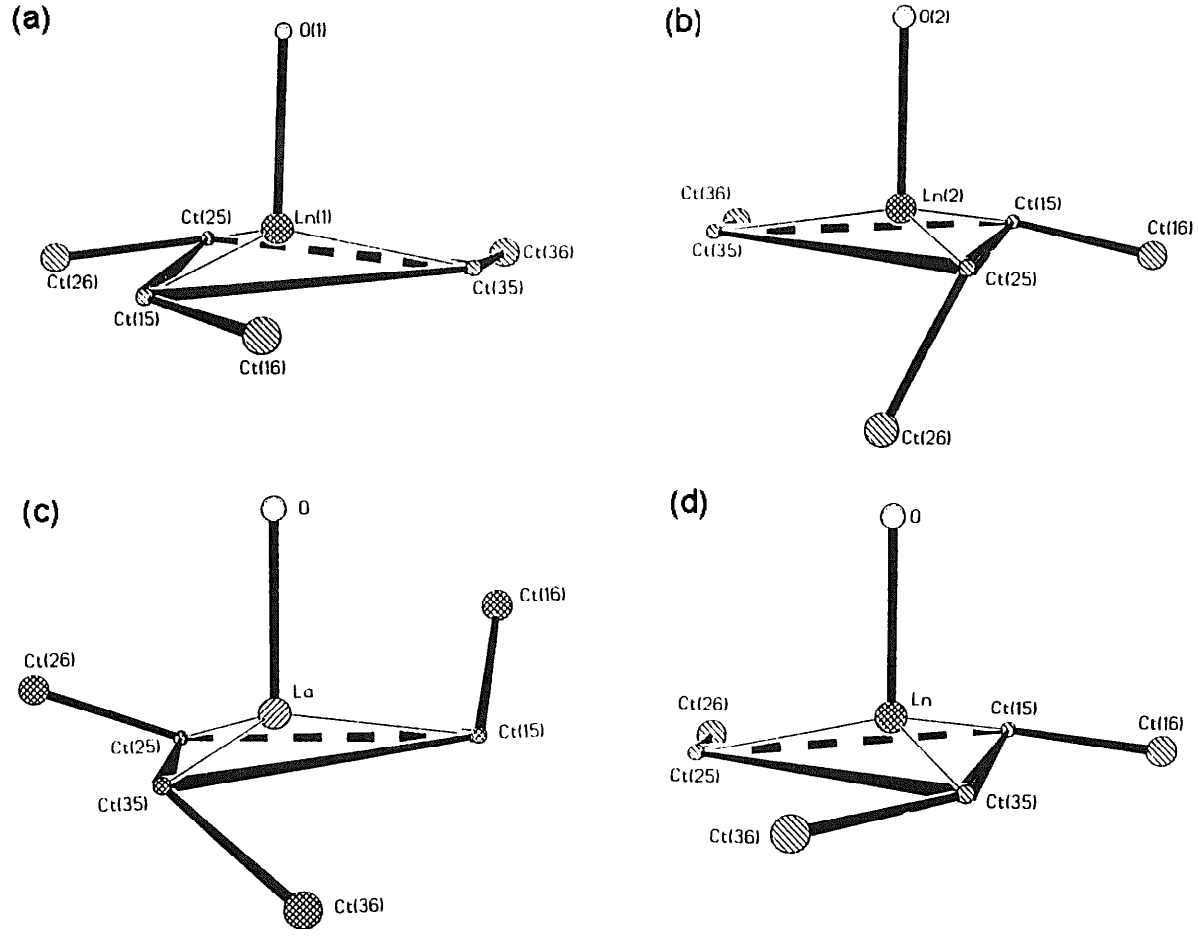

Fig. 1. Structure of motif I: (a) molecule a of motif I; (b) molecule b of motif I with atomic numbering schemes.

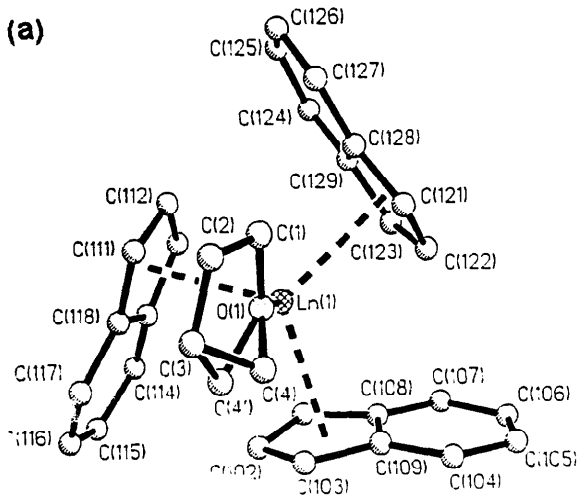

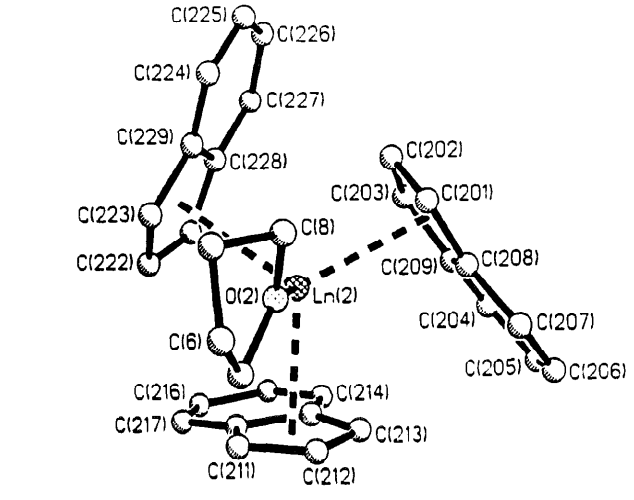

Fig. 2. Simplified view and comparison of the various conformations of motif I (a/b) (Ln = La, Pr, Nd); motif II (c) and motif III (d) (Ln = Nd, Sm), Ct*n*5 being the centres of the five-membered, Ct*n*6 of the six-membered ring of an indenyl ligand, respectively.

Table 4
Quantification of the various molecular conformations displayed by **1–4** (see Fig. 2a–d): Distances (in pm) of Ln and the various ring centres Ct*n*6, respectively, from the plane spanned by the three ring centres Ct*n*5 ($n = 1$–3). Negative distances refer to Ct*n*6 positions *below* the Ct*n*5 plane (i.e., Ln and O lie *above* that plane)

Sample	Ln	Molecule	Ln	Ct16	Ct26	Ct36
1a	La	a	504.2	−111.5	−154.7	−136.6
		b	418.9	−314.7	−1932.6	−138.4
1b			493.3	1572.6	884.4	−1313.8
2	Pr	a	497.6	−109.3	−180.2	−155.9
		b	422.6	−312.2	−1927.7	−150.7
3a	Nd	a	495.0	−147.6	−156.8	−152.4
		b	433.7	−312.2	−1934.6	−150.0
3b			507.1	−145.1	−145.1	−145.1
4	Sm		522.5	−154.5	−154.5	−154.5

*All measurements at room temperature except for **3b** (−120°C). Molecule a and b are defined as explained in the text.

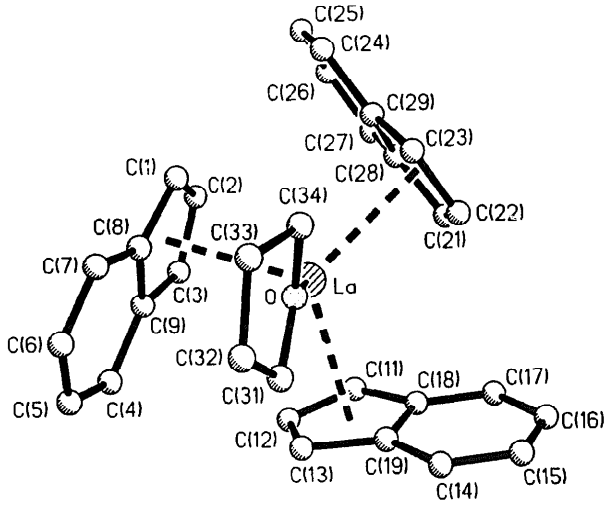

Fig. 3. Structure and atomic numbering scheme of sample **1b** (motif II).

throughout two high-field singlets result for the THF protons, and virtually four resonances at lower field for the C_9H_7 protons. The paramagnetic Ln^{3+} ions cause a quenching of *all* (Ln = Nd), or of *part* of the potential spin multiplets (Ln = Pr, Sm), while the C_9H_7 protons of **1** give rise to two quartets, one triplet and one doublet (Table 5, Fig. 5). The assignment of the signals of **1** follows that of the very similar NMR spectrum of the earlier-reported homologue with L = TPPO [10]. In view of **2–4** it has been assumed that by the paramagnetism of the ions Pr^{3+}, Nd^{3+} and Sm^{3+} the multiplets of the protons H-1/3 and H-2 will be quenched very readily, while the resonances of the more remote (from Ln) benzo protons H-5/6 and H-4/7 may retain, at least partially, their initial multiplet features.

A ^1H NMR pattern of four C_9H_7 resonances of the intensity ratio 6:6:6:3 would, in principle, agree with the

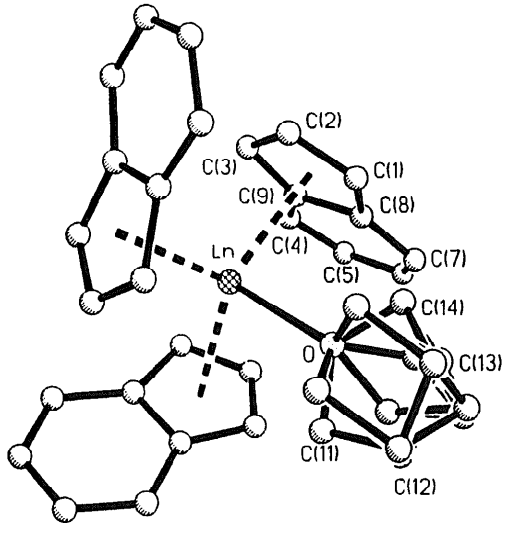

Fig. 4. Structure and atomic numbering scheme of as an example of a representative of motif III (Ln = Nd, Sm).

Table 5
Survey of ^{1}H NMR data obtained for C_6D_6 solutions of **1–4** at room temperature (δ in ppm; J in Hz)

Complex	Resonances of C_9H_7-protons				Resonances of THF	
	H-1/3	H-2	H-5/6	H-4/7	H(α)	H(β)
1 (La)	5.78(d, 6H) J = 3.16	5.81(t, 3H) J = 3.62; 3.1	7.14(q, 6H) $J \approx 3.1$	7.54(q, 6H) $J \approx 3.1$	3.13(s, 4H)	1.16(s, 4H)
2 (Pr)	9.39(s, 6H)	15.77(s, 3H)	6.39(q, 6H) $J \approx 3.0$	3.24(dd, 6H) J = 2.66; 3.34	−32.3(s, 4H)	−15.2(s, 4H)
3 (Nd)	6.42(s, 6H)	6.73(s, 3H)	5.42(s, 6H)	4.77(s, 6H)	−19.54(s, 4H)	−8.77(s, 4H)
4 (Sm)	11.52(s, 6H)	10.08(s, 3H)	7.62(q, 6H) $J \approx 3.0$	7.34(dd, 6H) $J \approx 2.7$; 3.36	−0.63(s, 4H)	−0.49(s, 4H)

assumption of three rapidly (on the NMR time scale) rotating, and hence in average strictly equivalent, indenyl ligands [10]. As **1** displays in toluene solution only one relatively sharp ($W_{1/2}$ = 508 Hz) ^{139}La resonance at −558.6 ppm, it seems justified here to assume 'unperturbed' η^5-coordination of all C_9H_7 ligands in solution, too. We have demonstrated earlier [24–26] that in CD_2Cl_2/CH_2Cl_2-solution adducts of the type $[La(\eta^5\text{-}C_5H_5)_3L]$ give rise to one high-field ^{139}La resonance between −508 and −578 ppm. Any change of the average ligand hapticity is clearly reflected by a displacement of the ^{139}La resonance towards higher or lower fields (Table 7). Thus, $\delta(^{139}La)$ of base-free $[La(C_9H_7)_3]$ in CD_2Cl_2 appears at −418 ppm ($W_{1/2}$ = 530 Hz) [27]. More recently, Windisch et al. [28] have shown that even partial replacement of cyclopentadienyl- by allyl ligands results in more drastical low-field shifts.

We wish to point out here that without any additional observation, the appearance of a four-resonance ^{1}H NMR spectrum for the protons of all three C_9H_7 ligands would be too poor an argument to postulate an all-η^5 coordination for **2–4**, too. Corresponding spectra have likewise been reported for the 'fast exchange

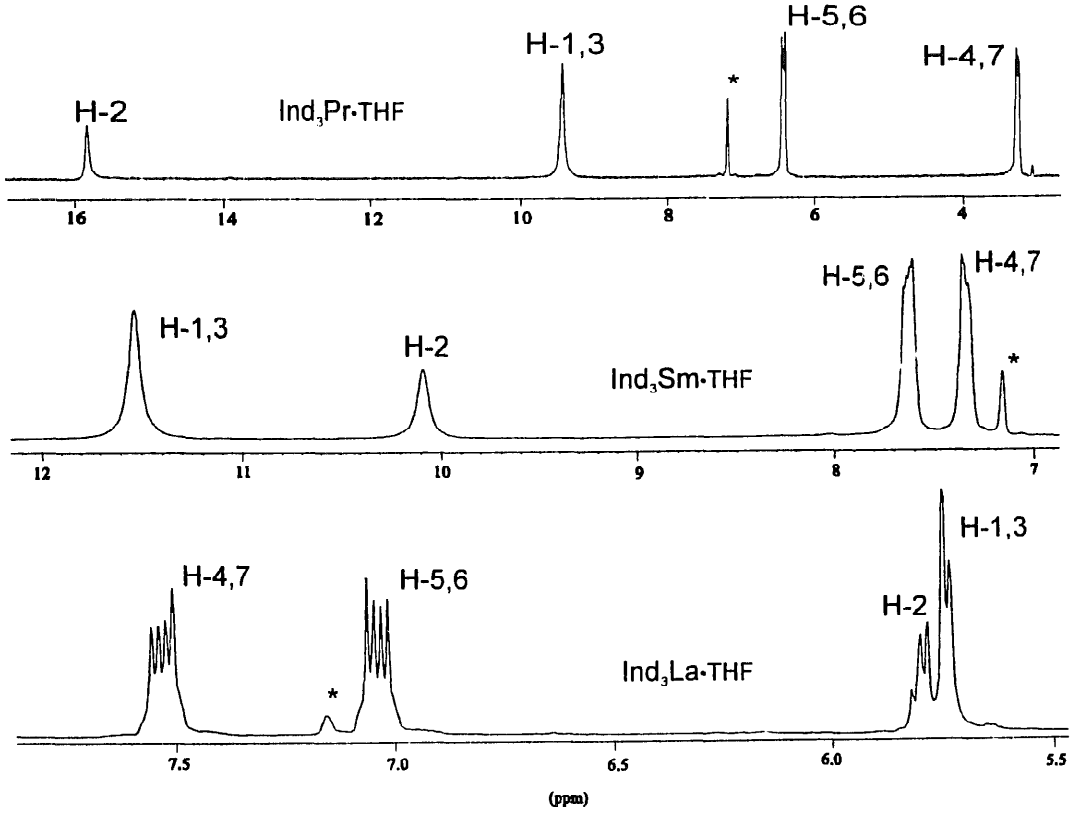

Fig. 5. Room temperature ^{1}H NMR spectra of (from top to bottom) **2**, **4** and **1**. The high-field sections displaying the two singlets of THF protons have been omitted, and the three δ-scales are drawn to different scales.

Table 6
Survey of structural work carried out on $[Ln(C_9H_7)_3THF]$ systems until now

Crystal	Ln	Motif	Crystal system	Space group	Z	Reference
1a		I	monoclinic	$P2_1/c$	8	
1b	La	II	monoclinic	$P2_1/c$	4	
1c		I	monoclinic	$P2_1/a$	8	Shen et al., unpublished
2	Pr	I	monoclinic	$P2_1/c$	8	
2a		I	monoclinic	$P2_1/a$	8	[12]
2b[a]		I	monoclinic	$P2_1/c$	8	
3a		I	monoclinic	$P2_1/c$	8	
3b	Nd	III	hexagonal	$P6_3$	2	
3c		III	hexagonal	$P6_3$	2	[11]
4	Sm	III	hexagonal	$P6_3$	2	
5	Gd	III	hexagonal	$P6_3$	2	[11]

[a]Crystal recovered from red, partially THF-free product (see text).

limit' of fluxional complexes involving C_9H_7 ligands reliably known to adopt η^1-coordination in the 'slow exchange limit' [29,30]. The residual multiplet splitting of one pair of benzo protons (most probably of H-4/7) of **2** and **4** into doublets of doublets might, inter alia, be indicative of any non-η^5-like 'low exchange limit'. Unfortunately, the solubility of **1–4** below room temperature in solvents 'chemically' suited for ^1H NMR spectroscopy has turned out to be too low to make use of VT-NMR spectroscopy.

In concluding this section, we wish to recall that the initially reported ^1H NMR spectrum of **4** [14,15] has long been considered as unusual in that its interpretation has led to the assumption of predominant η^1-coordination. While Deacon et al. have confirmed [31] the original NMR spectrum of **4** without, however, presenting any data, Vasamiliette [13] has observed, albeit without adding any details either, a spectrum apparently more reminiscent of that presented in Fig. 5. Numerous authors have, since 1969, referred to the occurrence of most probably η^1-bonded C_9H_7 ligands in **4**, which long-pending view [14,15] has, in our opinion, now become obsolete. We share Vasamiliette's statement

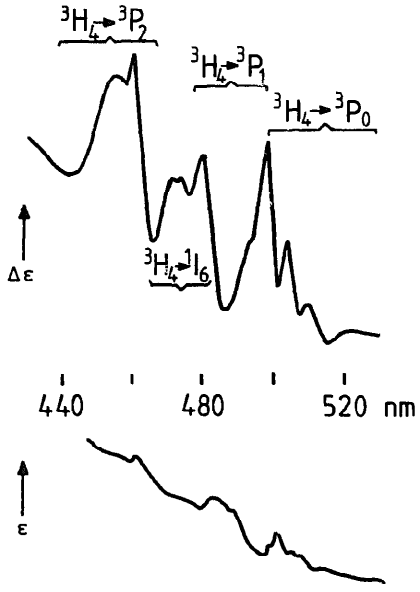

Fig. 6. Absorption spectrum (bottom), and magnetic circular dichroism (MCD) of **2** top between 440 and 520 nm (solvent: C_6H_6).

[13] that Tsutsui et al. most likely had studied partially decomposed samples and misinterpreted some resonances of free indene as part of the spectrum of **4**.

5.2. Optical (NIR / VIS) spectroscopy

As Amberger and Yünlü [16] have reported a study of the low-temperature NIR/VIS absorption and MCD (MCD = magnetic circular dichroism) spectra of **2** dissolved in 2-MeTHF, there might be some interest in the corresponding spectra of authentic **2** dissolved in C_6H_6 at room temperature. In Fig. 6, the regular absorption spectrum of **2** between 430 and 530 nm is compared with the corresponding MCD spectrum. While the f–f absorption spectrum of **2** suffers strongly from being superimposed on the low-energy wing of an intense CT transition (with its maximum below 430 nm), the corre-

Table 7
Dependence of $\delta(^{139}La)$ of the total (averaged) ligand hapticity and the charge of the complex

Sample	$\delta(^{139}La)$/ppm	$W_{1/2}$/Hz	Solvent	Reference
$[(C_5Me_5)La(C_3H_5)_2]$	13	> 1000	THF-d_8	[27]
$[Li(diox)_2][(C_9H_7)La(C_3H_5)_3]$[a]			THF-d_8	[27]
$[(C_5H_5)_2La(C_3H_5)]$	−214	1650	THF-d_8	[27]
$[(C_5H_4Me)_3La]$	−380	11800	CD_2Cl_2	[22]
$[(C_5H_5)_3La]_n$[b]			CD_2Cl_2	[22]
$[(C_9H_7)_3La]$	−418	530	CD_2Cl_2	[28]
$[Me_4N][(C_5H_5)_2LaF]$	−482	100	CD_2Cl_2	[22]
$[(C_9H_7)_3La \cdot THF]$	−558	508	C_7D_8	This work
$[(C_5H_5)_3La \cdot THF]$	−558	450	CD_2Cl_2	[22]
$[(C_5H_5)_3La \cdot DMSO]$	−564	22	C_7D_8	[25]
$[(C_5H_5)_3La(CNC_6H_{11})_2]$[c]	−614	550	CD_2Cl_2	[26]

[a]Diox = dioxane.
[b]Oligomeric (tetrameric) species in rapid equilibrium with mononuclear complex.
[c]Large excess of free c-$C_6H_{11}NC$.

sponding MCD spectrum is notably better structured. Actually, this MCD spectrum looks similar to the reported [16] MCD spectrum of **2**, which has been correlated successfully with the MCD spectrum of $[Pr(C_5H_5)_3$ THF] assuming all-η^5-coordination in both cases. Although considerable changes were observed on cooling that sample [16], it seems justified stating that also in solution **2** displays predominantly η^5-bonded indenyl ligands.

6. Experimental

6.1. General features

All manipulations had to be carried out under a strict atmosphere of pure nitrogen in making extensive use of familiar Schlenk techniques. All solvents were dried and distilled over Na–K alloy/benzophenone ketyl. Anhydrous lanthanoid trichlorides, $LnCl_3$, were prepared according to the literature [32], and NaC_9H_7 by treating indene with an excess of Na pearls in THF [14,15]. The lanthanoid content of **1–4** was determined by complexometric titration with EDTA, and the C/H content on a Heraeus CHN-O-Rapid analyser. Mass spectra were recorded on a Varian type 311A instrument with a Spectrosystem MAT 188 (Finnigan) detector, IR spectra on a Perkin–Elmer 1720 FT-IR spectrometer, and ^1H NMR spectra on a Varian Gemini 200 MHz instrument. The ^{139}La NMR-spectrum was obtained on a Bruker AM 360 spectrometer. This spectrum was recorded at room temperature in a 3:7 mixture of $CD_3C_6D_5$ and $CH_3C_6H_5$, using a 10 mm-NMR-tube under the following conditions: Deuterium lock, SI = 4 K, TD = 8 K, SW = 71 kHz, DW = 7.0 μs, AQ = 0.05 s, NS = 825. A solution of $LaCl_3$ in D_2O was used as the external standard, for which $\delta(^{139}La) \equiv 0$ ppm.

6.2. Preparation of $[(C_9H_7)_3Ln \cdot THF]$ 1–4

The preparation of all *four* complexes, **1–4**, was, in its initial phase, analogous to the procedure given in the literature [14,15], i.e., anhydrous $LnCl_3$ was reacted with NaC_9H_7 in THF in the ratio 1:3 for 1–2 days at room temperature, but thereafter, the reaction mixture was refluxed for another 3 to 4 days. After NaCl-removal by centrifugation, solvent evaporation and drying, the residue was dissolved again in a large amount of refluxing toluene, and the hot supernatant was filtrated instantaneously. After several repeatedly continued extractions, the solution in total was concentrated and cooled down to ca. 0°C, whereafter the pure product of $[(C_9H_7)_3Ln \cdot THF]$ could be collected as microcrystals or as a powder. The analytically pure product (see Table 1) was dissolved either in pure toluene, pure THF, or in a toluene/THF-mixture (with toluene in large excess), from which solutions single crystals suitable for crystallographic X-ray studies were obtained.

6.3. X-ray crystallography

Selected single crystals of **1–4** were positioned in carefully conditioned, and finally sealed, thin-walled Lindemann capillaries for the room temperature X-ray studies, or coated by a viscous polyfluorpolyethylene oil for the measurement at low temperature. The Laue symmetry and crystal orientations were determined by standard techniques making use of X-ray photographs similar to those described by Churchill et al. [33] on the Syntex $P2_1$ instrument (at room temperature), or on the Hilger & Watts four-circle-diffractometer (at lower temperature). From photographs taken along different axes, the unit cell parameters could most be reliably duced. Details of relevance for the data collection and refinement are given in Table 2. All calculations were carried out using the SHELX-93 and SHELXTL-PLUS program sets [34]. Heavy atoms were found from Patterson maps or located through direct method, and other non-hydrogen atoms were detected by Fourier techniques. The structures were refined by full-matrix least-squares techniques. Hydrogen atoms were included using a riding model with d(C–H) = 96 pm. Final refinement of position and anisotropic thermal parameters (one unique isotropic parameter, with free choice for all hydrogen atoms only) converged to the final R values given in Table 2. The atomic coordinates of **1–4** and further details of the crystal structure investigation may be obtained from the Fachinformationszentrum Karlsruhe, D-76344 Eggenstein–Leopoldshafen, Germany on quoting the depository number CSD-407088 for **1a**; CSD-407085 for **1b**; CSD-407090 for **2**; CSD-407086 for **3a**; CSD-407087 for **3b** and CSD-407089 for **4**. Detail information and data concerning the structure analysis of crystal **1c** are available on request from Prof. Q. Shen.

Acknowledgements

The authors express their gratitude to the Friedrich–Ebert–Stiftung (Bonn) for the generous donation of a fellowship to J. Guan, and to Professor U. Behrens (Hamburg) for his kind assistance to overcome numerous problems during the crystallographic studies.

References

[1] M. Adam, U. Behrens, R.D. Fischer, Acta Crystallogr. C47 (1991) 968, and references therein.
[2] V.K. Belsky, K.Yu. Gunko, G.L. Solveichik, B.M. Bulychev, Metalloorg. Khim. 4 (1991) 577.

[3] V.K. Belsky, K.Yu. Gunko, G.L. Solveichik, B.M. Bulychev, Organomet. Chem. USSR 4 (1991) 281.
[4] H. Schumann, J.A. Meese-Marktscheffel, L. Esser, Chem. Rev. 95 (1995) 865, comprehensive review.
[5] R. Maier, B. Kanellakopulos, C. Apostolidis, B. Nuber, J. Organomet. Chem. 435 (1992) 275, and references therein.
[6] Z. Wu, Z. Xu, X. You, X. Zhou, X. Huang, J. Chen, Polyhedron 13 (1994) 379.
[7] W. Chen, G. Lin, J. Xia, G. Wei, Y. Zhang, Z. Jin, J. Organomet. Chem. 467 (1994) 75.
[8] S. Wang, Y. Yu, Z. Ye, C. Qian, X. Huang, J. Organomet. Chem. 464 (1994) 55.
[9] J.L. Atwood, J.H. Burns, P.G. Laubereau, J. Am. Chem. Soc. 95 (1973) 1830.
[10] J. Guan, R.D. Fischer, J. Organomet. Chem. 532 (1997) 147.
[11] J. Xia, Z. Jin, G. Lin, W. Chen, J. Organomet. Chem. 408 (1991) 173.
[12] S. Wang, D. Kong, Z. Ye, X. Huang, J. Organomet. Chem. 496 (1995) 37.
[13] J.-L. Vasamiliette, PhD Thesis, Université de Liège, Liège, Belgium, 1987.
[14] M. Tsutui, H.J. Gysling, J. Am. Chem. Soc. 90 (1968) 6880.
[15] M. Tsutui, H.J. Gysling, J. Am. Chem. Soc. 91 (1969) 3175.
[16] H.-D. Amberger, K. Yünlü, Spectrochim. Acta 42a (1986) 393.
[17] Z. Huang, R. Cai, W. Wu, W. Qiu, J. Fudan Univ. Nat. Sci. Edn. 24 (1985) 476.
[18] Z. Ye, S. Wang, D. Kong, X. Huang, J. Organomet. Chem. 491 (1995) 57.
[19] M. Chen, G. Wu, W. Wu, S. Zhuang, Z. Huang, Organometallics 7 (1988) 802.
[20] Y. Su, Z. Jin, W. Chen, J. Chin. Rare Earth Soc. 2 (1990) 106.
[21] W. Chen, S. Xiao, Y. Wang, G. Yu, Kexue Tongbao 22 (1983) 1370.
[22] S.H. Eggers, J. Kopf, R.D. Fischer, Organometallics 5 (1986) 383.
[23] H.G. Brittain, in: Lanthanide probes in life, chemical and earth sciences, J.-C.G. Bünzli, G.R. Choppin (Eds.), Elsevier, Amsterdam, 1989, 295.
[24] S.H. Eggers, M. Adam, E.T.K. Haupt, R.D. Fischer, Inorg. Chim. Acta 139 (1987) 315.
[25] S.H. Eggers, R.D. Fischer, J. Organomet. Chem. 315 (1986) C61.
[26] M. Adam, E.T.K. Haupt, R.D. Fischer, Bull. Magn. Reson. 12 (1990) 101.
[27] M. Adam, Doctoral Dissertation, Universität Hamburg, Germany, 1990, p. 10.
[28] H. Windisch, J. Scholz, R. Taube, B. Wrackmeyer, J. Organomet. Chem. 520 (1996) 23.
[29] F.A. Cotton, T.J. Marks, J. Am. Chem. Soc. 91 (1969) 3178.
[30] P.E. Rakita, A. Davison, Inorg. Chem. 8 (1969) 1164.
[31] G.B. Deacon, R.H. Newnham, Aust. J. Chem. 38 (1985) 1757.
[32] M.D. Taylor, C.P. Carter, J. Inorg. Nucl. Chem. 24 (1962) 387.
[33] M.R. Churchill, R.A. Lashewycz, F.J. Rotella, Inorg. Chem. 16 (1977) 265.
[34] G.M., Sheldrick, SHELX-86, Acta Crystallogr., A46 (1990) 467; SHELX-93, Program for the Refinement of Crystal Structures, Universität Göttingen, Germany, 1993; SHELX-PLUS, Release 4.21/v, Siemens Analytical X-ray Instruments, Madison, WI.